

In Situ Assembly of DNA/Graphene Oxide Nanoplates to Reduce the Fire Threat of Flexible Foams

*Original*

In Situ Assembly of DNA/Graphene Oxide Nanoplates to Reduce the Fire Threat of Flexible Foams / Maddalena, Lorenza; Carosio, Federico; Fina, Alberto. - In: ADVANCED MATERIALS INTERFACES. - ISSN 2196-7350. - ELETTRONICO. - 8:(2021). [10.1002/admi.202101083]

*Availability:*

This version is available at: 11583/2971336 since: 2022-09-16T07:17:37Z

*Publisher:*

Wiley

*Published*

DOI:10.1002/admi.202101083

*Terms of use:*

This article is made available under terms and conditions as specified in the corresponding bibliographic description in the repository

*Publisher copyright*

(Article begins on next page)

# In Situ Assembly of DNA/Graphene Oxide Nanoplates to Reduce the Fire Threat of Flexible Foams

Lorenza Maddalena, Federico Carosio,\* and Alberto Fina

The layer-by-layer surface modification of open cell foams is a recently developed route to reduce the fire threat of this class of materials. This approach generally requires a high number of deposition steps to achieve the desired properties. This paper reports the water-based single-step deposition of efficient flame retardant coatings encompassing graphene oxide (GO) and DNA. During the deposition, a temperature-induced in situ assembly of the GO+DNA produces a continuous and thermally robust protective layer on the structure of the polyurethane (PU) foam where GO nanoplates are held together by DNA acting as a ligand. This GO+DNA coating can effectively prevent flame spread during flammability tests performed in horizontal or vertical configuration while considerably reducing the rate of combustion and production of smoke by cone calorimetry (−75% and 30% in peak of heat release rate and total smoke release, respectively). The DNA promotes the formation of a protective structure that efficiently limits heat and volatiles transfer from and to the flame thus resulting in flame retardant (FR) performances capable of outperforming many of the FR coatings developed so far for PU foams. The proposed approach potentially opens up to the development of high performing FR solutions based on graphene-related materials and bio-based components.

extensively used with good results in terms of flame retardancy performance. Phosphorus-containing additives (including organophosphate, organophosphonates, halophosphonates, phosphine oxides, and red phosphorous) and nitrogen-based flame retardant additives (i.e., melamine, urea, and dicyanamide) were also used as fire retardants for PU.<sup>[3–8]</sup> However, recent awareness concerning possible toxicological and environmental risks associated with the use of such FR chemicals have pointed out the need for the development of new, safe, and performing solutions.<sup>[9,10]</sup>


Lower flammability foams produced from bio-based resources such as alginates, nanocellulose, and cellulose fibers have also been proposed as possible FR alternatives.<sup>[11–15]</sup> However, the production processes of these foams need to be further developed to match the requirements for practical scale applications.<sup>[16]</sup> Alternatively, the surface modification of PU foams has been proposed as a practicable route for the preparation of flame retarded foams capable of addressing the needs for sustainable, nontoxic, and high-performing materials.<sup>[17]</sup> Indeed, owing to the high amount of exposed surface per volume unit of open cell PU foams, the use of a surface approach has been demonstrated to be particularly convenient to confer flame retardancy to this type of materials.<sup>[18]</sup>

For example, graphene-related materials have been successfully exploited for the design of efficient FR coatings when deposited in combination with montmorillonite clay,<sup>[19]</sup> polydopamine,<sup>[20]</sup> ammonium polyphosphate, and silicone resins.<sup>[21–24]</sup> A recent approach involving the synthesis of novel co-polymers has been demonstrated capable of conferring improved adhesion, superhydrophobicity and fire retardant properties.<sup>[25]</sup> In this context, the layer-by-layer (LbL) approach has been demonstrated to be a versatile option for the preparation of flame retarded textiles, foams, and films,<sup>[26–28]</sup> owing to the possibility to deposit coatings with different thickness and compositions as a function of the process parameters and selected reagents.<sup>[29–33]</sup> One of the most successful and used FR-coating formulation relies on the use of nanoparticles in combination with a polyelectrolyte matrix.<sup>[34]</sup> In particular, plate-shaped nanoclays such as montmorillonite and vermiculite have been widely used in LbL flame retardant coatings because of their high aspect ratios and their thermal stability, yielding FR coatings capable of shielding heat and reduce volatile release.<sup>[35–37]</sup> Most recently, graphene-related materials have been successfully exploited in water-based LbL

## 1. Introduction

Flexible polymer foams (typically polyurethanes, PU) are widely exploited materials in transports and buildings, owing to their use as the main constituent for upholstered furniture, sound proofing, and thermal insulation panels. Unfortunately, their organic characteristic coupled with their low density makes PU foams extremely flammable and one of the first items to be ignited during a fire.<sup>[1]</sup> The common approach to solve this problem is to use flame retardant (FR) chemicals that are normally incorporated within the foam structure during the foaming process and can provide a certain degree of fire retardancy in building and transport applications.<sup>[2]</sup> To this aim, halogen-based flame retardant agents have been

L. Maddalena, F. Carosio, A. Fina  
Politecnico di Torino-Alessandria Campus  
Via Teresa Michel 5, Alessandria 10121, Italy  
E-mail: federico.carosio@polito.it

 The ORCID identification number(s) for the author(s) of this article can be found under <https://doi.org/10.1002/admi.202101083>.

© 2021 The Authors. Advanced Materials Interfaces published by Wiley-VCH GmbH. This is an open access article under the terms of the Creative Commons Attribution License, which permits use, distribution and reproduction in any medium, provided the original work is properly cited.

DOI: 10.1002/admi.202101083

assemblies, typically exploiting the oxidized nanoplates (GO).<sup>[38]</sup> Indeed, GO is negatively charged in water, mainly because of the carboxylic groups obtained by exposing graphene to strong oxidizers, allowing GO stabilization in water.<sup>[39]</sup>

LbL structures comprising a positively charged polyelectrolyte and high aspect ratio graphene oxide (GO) platelets have been assembled as flame retardant coating on open cell PU foams.<sup>[40–42]</sup> For example, a chitosan (CHIT)/GO assembly was reported to completely coat the 3D structure of PU foams yielding a continuous coating capable of protecting the foam toward flame application and heat flux.<sup>[41]</sup> A three bilayer (BL) coating easily prevented the collapsing of the foam structure during combustion thus suppressing the melt dripping typical of PU foams and considerably reducing the rate of combustion, as demonstrated by flammability and cone calorimetry tests, respectively. In addition, increasing the number of deposited BL to 6 further limited the ignitability of the foams, by reducing volatiles emission below flammability limits. The inclusion of a phosphate salt within the coating formulation in order to control the ionic strength has been proven to increase the thickness of the deposited coatings while conferring additional flame retardant features to the coated foams. It was, indeed, proved that only three BL were required for achieving self-extinguishment by flammability tests and completely preventing the ignition of the foam by cone calorimetry tests.<sup>[42]</sup>

From the comparison of the results reported in the literature, it is suggested that the performance of the FR action of nanoplates-based coatings is strongly dependent on their lateral size.<sup>[40]</sup> Indeed, high aspect ratio nanoplates have a higher probability to overlap more efficiently, with respect to low aspect ratio ones, and produce an effective barrier to volatiles and heat with fewer deposition steps.<sup>[43,44]</sup> Although the use of high aspect ratio nanoparticles is capable of considerably improving the efficiency of the achieved FR coatings, these coatings still suffer from limited upscalability owing to the time-consuming nature of the process.<sup>[45]</sup> In addition, the high volume of solution required coupled with the large volume of washing water, used to avoid cross contaminations, further adds practical constraints to this FR approach. To address these limitations, in the present paper we report the single-step deposition of a highly ordered flame retardant coating based on deoxyribonucleic acid (DNA) and GO for the protection of PU foams (Figure 1).

The GO nanoplates are the main constituent of the coating while DNA acts as a ligand between nanoplates. DNA is a macromolecule formed by nucleotides covalently bonded to forming polynucleotides arranged in double helix. Each nucleotide, composed of a unit of deoxyribose carrying a phosphate group and a nitrogen containing nucleobase, is bonded to another by a phosphor-diester linkage between the sugar of one nucleotides and the phosphate of the next resulting in an alternating sugar-phosphate backbone. The double helix is obtained by the hydrogen bond stored between the nitrogen containing nucleobases of two separate polynucleotides.<sup>[46]</sup> In this configuration, DNA is negatively charged in water because of the deprotonation of phosphate groups not involved in the phosphor-diester linkage. However, when the DNA is denatured by heating, the double strand is opened thus allowing the exposure of nitrogen bases that can be protonated in acidic condition. This produces positive charges on the DNA that can then complex with GO carboxylic functionalization.<sup>[47]</sup> The use of proteins and nucleic acids as FR chemicals has been recently demonstrated as viable route for the development of FR solutions for textiles and plastics owing to the intrinsic intumescent features of this kind of bio-macromolecules.<sup>[48–50]</sup> In particular, DNA has been presented as an all-in one intumescent system as in its structure it is possible to find the three main components of an intumescent formulation (i.e., acid source from the phosphate, blowing agent from the nitrogen containing bases, and carbon source from the deoxyribose backbone).<sup>[51]</sup> Here, DNA is used as functional “mortar” capable of reacting to the exposure to heat and flame and produce a stable carbonaceous structure holding together the GO nanoplates thus resulting in the production of a barrier to heat and volatiles. The morphology of the coatings was evaluated by field emission scanning electron microscopy. The reaction to fire was tested by horizontal and vertical flammability tests. Foams coated with this GO+DNA coating showed no ignition during flammability test in both horizontal and vertical configurations while also considerably reducing the combustion rates and smoke released during forced combustion tests. These results clearly show the superior FR properties of the coatings developed in this paper that could open up for the design of advanced FR materials in a plethora of application fields.

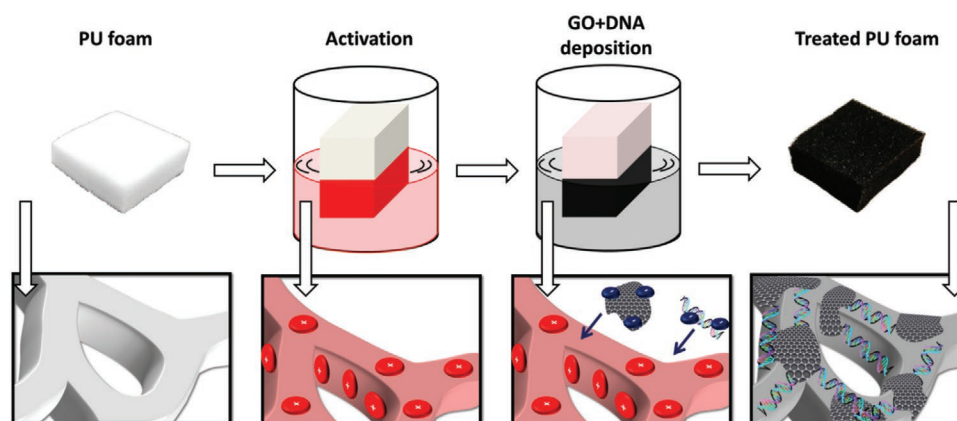


**Figure 1.** Schematic representation of the single-step deposition. PU foams are previously activated and then dipped in negative GO-based suspension.

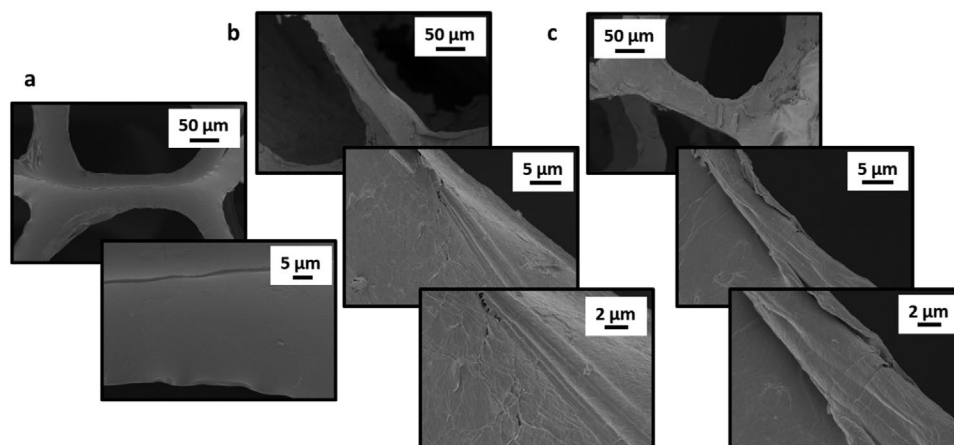


Figure 2. SEM images of a) PU, b) PU GO, and c) PU GO+DNA samples.

## 2. Results and Discussion

### 2.1. Coating Morphology

The morphology of the deposited coatings was evaluated by field emission scanning electron microscopy (FESEM). **Figure 2** reports collected microscopy images of neat PU, PU GO, and PU GO+DNA.

Neat PU shows the typical structure of an open cell with open pores and cell walls (Figure 2a). The morphology of these latter reveals a smooth surface where wrinkled irregularities resulting from the foaming process can be detected mostly at the edges. The one-step deposition of PU GO (Figure 2b) significantly changes the morphology of neat PU foam without modifying its open cell nature. Indeed, high-magnification microscopy images clearly show the formation of a wrinkled morphology that can be associated to the overlap of GO nanoplates.<sup>[40–42]</sup> The surface appears rougher compared to PU, with clearly visible GO boundaries. In contrast, when GO+DNA is deposited, the resulting surface appears smoother and more homogeneous, likely because of the presence of DNA acting as ligand between GO nanoplates. In the adopted deposition conditions, the acidic pH of the used GO suspension coupled with the temperature allow for the formation of in situ GO+DNA complexes via strong noncovalent interactions which deposition is forced upon solvent removal.<sup>[47]</sup> Indeed, it is well-known that DNA will denature opening up the double strand in the 60–80 °C thus exposing the nitrogen rich bases that are then protonated by the naturally acidic pH of the GO suspension (pH 2).<sup>[52]</sup> This produces positive charges on the DNA that can then complex with GO carboxylic functionalization.<sup>[47]</sup> This was further demonstrated by putting ≈10 mL of water-based GO+DNA dispersion in a closed vessel and heating it in oven at 70 °C overnight obtaining a stable gel (Figure S2, Supporting Information). As a control sample, the same procedure was applied to the GO suspension, in which gelation did not occur. These results are in agreement with the literature background describing the preparation of GO/DNA networks.<sup>[47]</sup>

### 2.2. Flame Retardant Characterization and Residues Analysis

The flame retardant properties of treated foams were tested by means of cone calorimetry and flammability test. The combination of these methods provides an exhaustive set of information about the contribution of a material in both initiating a fire, after a small flame application (flammability test), or propagating it when exposed to a heat flux typical of developing fires (cone calorimetry test). To evaluate the effects of a combined DNA/GO coating, a PU sample coated by just DNA is also prepared and tested. **Figures 3** and **4** show pictures from flammability and parameters collected from cone calorimetry tests, respectively, whereas Tables S1 and S2 (Supporting Information) report numerical data collected while performing tests.

Flammability tests in horizontal configuration showed a small flame applied to the neat PU foam is sufficient for almost instantaneous ignition and quick consumption by the flames, with release of incandescent and low viscous molten droplets, able to ignite the dry-cotton placed under the foam. This phenomenon is called melt-dripping, and it is a typical fire risk of synthetic polymers because it leads to fire propagation.<sup>[53]</sup> The deposition of DNA can suppress the melt-dripping phenomenon but cannot stop flame spread. Indeed, after methane flame application, the sample is completely consumed by the flame burning vigorously leaving a residue accounting for the 8% of the initial weight. In contrast, the deposition of the GO-based coating dramatically changes the PU flammability. Indeed, when the flame is applied to the GO-treated foam, ignition occurs, but the flame slowly spreads within the first centimeter of the sample, without showing melt-dripping, and it is eventually extinguished after an average flaming time of 8 s. The final residue is extremely high and accounts for ≈99% of the initial sample weight. The DNA inclusion within the coating further improves the flame retardant properties. Surprisingly, a nearly instantaneous self-extinguishment upon the removal of the Bunsen methane flame occurred thus indicating that the ignition was prevented.

The flammability behavior of the GO-containing samples was also tested in vertical configuration that it is normally considered a harsher testing setup, compared to the horizontal

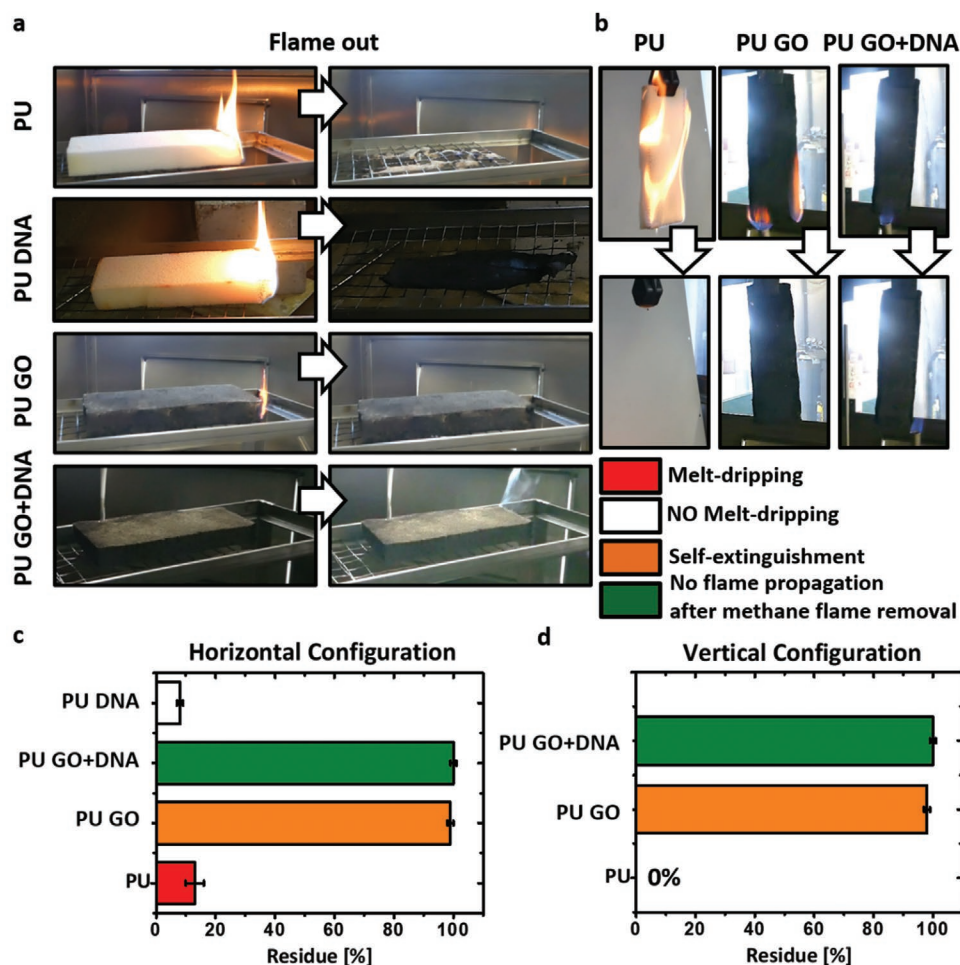


**Figure 3.** Snapshots from flammability test in a) horizontal and b) vertical configuration of untreated versus coated foams. End-of-test residues and flammability behavior in c) horizontal and d) vertical configuration.

test. In this condition, the pristine PU ignites immediately after the flame application and the flame reaches the top of the sample in only 2 s triggering the melt-dripping phenomenon that causes the collapsing of the entire sample. The deposition of GO nanoplates can prevent flame spread, suppress melt-dripping, and achieve a self-extinguishing behavior with an average after-flame time of 5 s. The residue collected at the end of the test shows limited damage and account 98% of residue. In addition, the inclusion of DNA as ligand for GO nanoplates completely prevents ignition as already observed in horizontal configuration. This extraordinary performance is maintained even after multiple flame applications, thus pointing out the superior FR properties of this GO+DNA coating. The obtained result is comparable with what previously reported in literature for LBL coatings, comprising multiwalled carbon nanotubes (MWCNT).<sup>[54]</sup> In that work, Holder and collaborators showed the efficiency of MWCNT to produce a robust char layer able to prevent the flame spread in vertical flame test after one flame application. However, that result was obtained by depositing 9BL of branched polyethylenimine functionalized with pyrene (BPEI+Pyr) assembled with a dispersion of MWCNT in polyacrylic acid (PAA+MWCNT), reaching a 44% of weight gain, thus resulting in a very laborious process. In contrast, the

single deposition proposed in this paper allowed to reach ~80% of weight gain and flame spread prevention for four consecutive flame applications. The performed tests proved the effectiveness of the deposited coating as flame retardant solution for PU foams toward the direct flame application. However, besides the presented advantages in terms of flammability, in a developing fire scenario, PU foams are typically subjected to a radiative heat flux generated from a flame, which corresponds to a different testing condition. Indeed, forced combustion tests by cone calorimetry were performed to further analyze the reaction of pristine and coated PU foams to a radiative heat flux thus evaluating their contribution to fire development. Plots from cone calorimetry tests are reported in Figure 4 while the main parameters are collected in Table S2 (Supporting Information).

During a cone calorimeter test, the sample is exposed to a heat flux produced by a conical heater delivering an incoming heat flux to the sample of  $35 \text{ kW m}^{-2}$  that represents early stages of a developing fire.<sup>[55]</sup> The applied heat flux triggers the decomposition of the sample and the release of flammable volatiles. In these conditions, PU quickly ignites and burns vigorously reaching a peak of heat release rate (pkHRR) of about  $304 \text{ kW m}^{-2}$ . During combustion the foam structure collapses

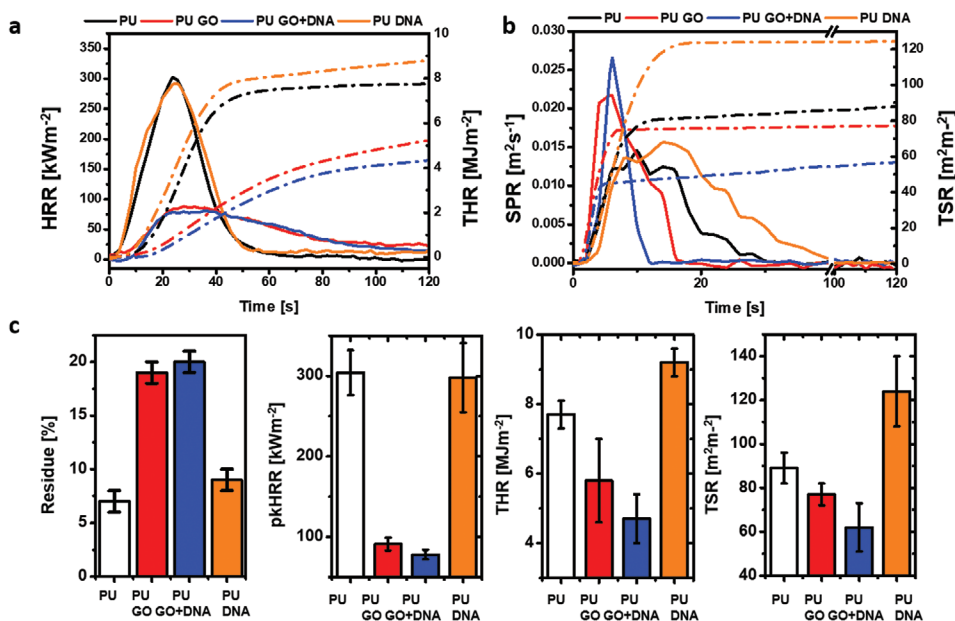


**Figure 4.** a) Heat release rate (HRR, solid line) versus time and total heat release versus time (THR, dotted line), b) smoke production rate (SPR, solid line) versus time and total smoke release versus time plots (TSR, dotted line), and c) residues, peak of heat release rate (pkHRR), total heat release rate (THR), and total smoke release comparison of tested samples (TSR).

leaving a pool of a low viscosity liquid that is responsible for the steeply increase in heat release rate (HRR).<sup>[53]</sup> The final residue accounts for 7% of the original weight and is mainly ascribed to inorganic additives used during foam production. As observed for flammability, the presence of a DNA coating does not yield substantial improvements in the PU burning behavior. Indeed, no effects on HRR are observed, whereas total heat release rate (THR) and total smoke release (TSR) values are increased owing to the presence of the coating organic components. Conversely, the GO coating increases the ignition time and considerably lowers the combustion rates as demonstrated by a 70% reduction in pkHRR. These performances are improved by the presence of DNA that can further reduce the pkHRR (−75%, compared to PU). This trend is also observed for smoke parameters, where the GO+DNA coating achieves a 30% reduction in TSR, compared to neat PU, whereas the GO coating only reduces this parameter by 13%. It is apparent that both GO coatings can dramatically change the combustion behavior of the foam. Indeed, the treated PU no longer collapses and maintains its original shape, slightly shrinking as the combustion proceeds. This is ascribed to the presence of the coating that, by extending through the entire thickness of the foam as protective exoskeleton, can mechanically sustain the structure. Then, the highly oriented GO nanoplates produce a barrier that hinders the release of combustible volatiles thus decreasing fuel feeding the flame. In addition, the presence of GO nanoplates might also re-radiate a portion of the heat reaching the foam, thus reducing the net incoming heat flux for polymer decomposition, directly affecting the production of flammable volatiles. This mechanism is valid for both GO and GO+DNA coatings. However, as already discussed for flammability tests, the presence of DNA further improves the FR owing to its intrinsic intumescent features that help in binding the GO nanoplates

together and build a more efficient barrier. In addition, the tests performed on foams treated by only DNA further demonstrated the crucial role of the DNA/GO complex in the FR behavior of the coating. To prove these hypotheses the residues collected at the end of combustion were imaged by SEM and analyzed by Raman spectroscopy as reported in **Figure 5**.

SEM investigations performed on the cross sections of the residues clearly show that both GO and GO+DNA coatings were capable of maintaining the original 3D structure of the foam (Figure S3, Supporting Information). PU GO samples evidence the formation of a thermally stable protective layer, confirming the propensity of GO nanoplates to act as physical barrier toward flames and volatiles (Figure 5a). However, the obtained carbonaceous residue is brittle as several cracks are visible. In contrast, the morphology of the PU GO+DNA residue closely resembles the one of the uncombusted samples and exhibits a thick hollow structure with exposed GO nanoplates. Interestingly, high-magnification images evidenced a swelling of the stacked GO that can be ascribed to the intrinsic intumescent flame retardant action of DNA (Figure 5b). Raman spectroscopy confirms the presence of two distinct signals at 1605 and 1350  $\text{cm}^{-1}$  attributed to the bands generally labeled as G and D, respectively (Figure 5c). As reported in literature, the D band is normally associated to the number, the type and the distance between defects in graphene-related materials (disordered structures) while G is associated to the breathing mode of the aromatic plane (ordered structures).<sup>[56–58]</sup> To evaluate the evolution of the carbon structure formed during combustion, the ratio between the area underneath these two bands was considered. Because of Raman spectra collect only relative spectra, the band parameters strongly depends on the recorded intensity (i.e., counts), in contrast the band areas ( $D_A$  and  $G_A$ ) is a function of both peak intensity and FWHM; therefore, the

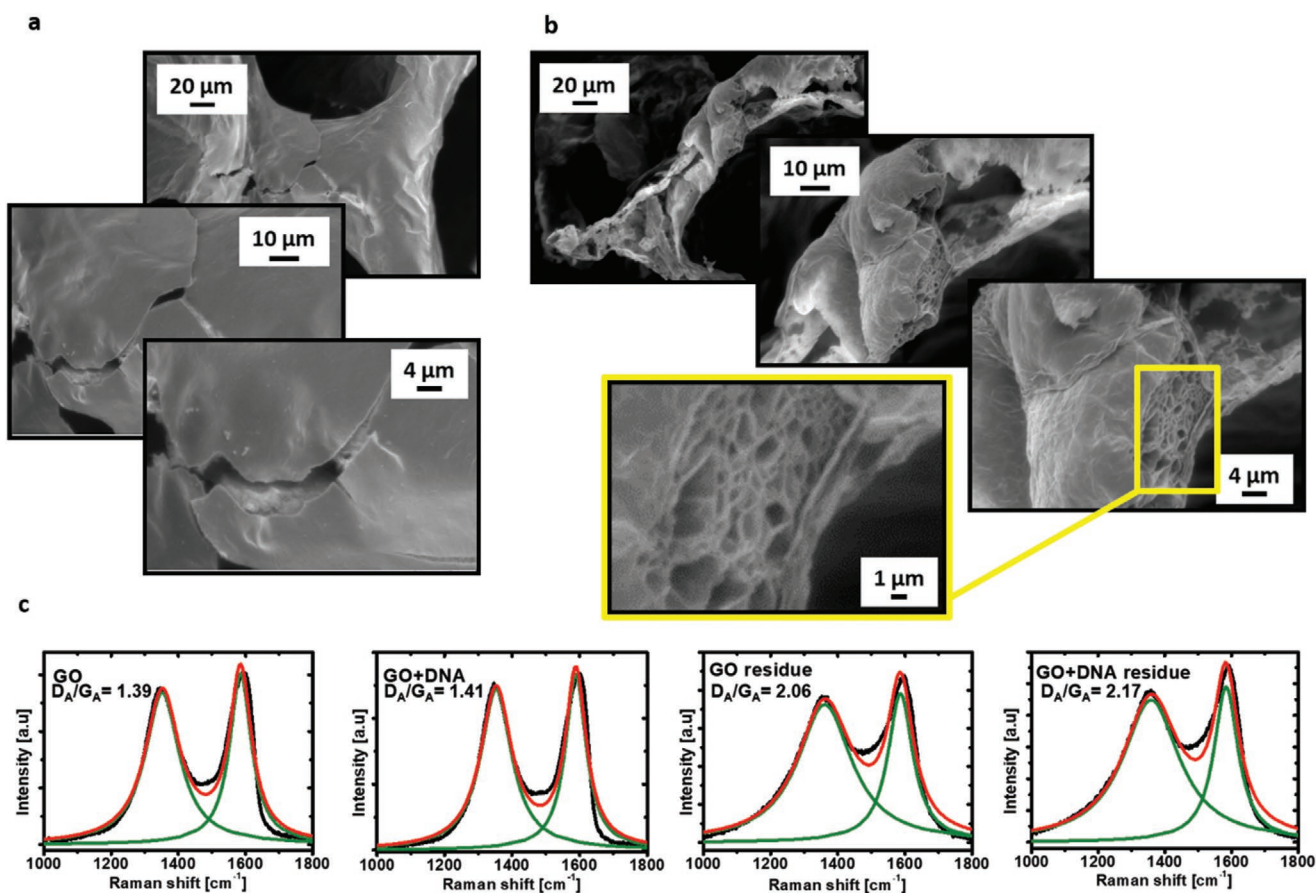


**Figure 5.** Post combustion residue analysis: SEM image performed on the cross sections of a) PU GO and b) PU GO+DNA residues after cone calorimetry test and (c) Raman spectra of single-step deposited sample before and after exposure to cone calorimetry

bands area can be used for better characterize the order of the obtained char.<sup>[59,60]</sup>

The as-deposited samples yielded similar values likely owing to the presence of GO as the main components contributing to Raman signal. Conversely, residues show higher  $D_A/G_A$  compared to uncombusted samples as a consequence of the formation of amorphous carbon during PU decomposition or by the partial oxidation of GO, overall leading to a broadening of the D band. This is apparent for PU GO+DNA residue that showed the highest  $D_A/G_A$  ratio likely due to the presence amorphous char produced by DNA.

Comparing the obtained results with the existing literature on LbL coatings comprising 3D and 2D nanoparticles like graphene-related materials, it is apparent that the single-step deposition presented in this paper can achieve overall higher FR performances with only one deposited layer (Figure 6). Indeed, while most of the previously reported LbL coatings can easily achieve substantial reductions in pkHRR, most of them fail in preventing flame spread in either horizontal or vertical configuration. The related clear advantage of the single-step deposition method developed in this paper appears to be related to the high add-on achieved. As an example, GO and GO+DNA treated PU foams yield a weight gain about four times higher than the amount of BPEI/GO+sodium alginate (SA) coating, which correspond to the 25% wt after 24 deposition steps.<sup>[61]</sup>

In addition, the proposed coating procedure has been found to provide excellent flame retardant properties even when compared with recently developed strategies that rely on organic solvents to deposit efficient flame retardant silicone and silicone/GO coatings.<sup>[18,23,24]</sup> These comparisons underline the effectiveness of the proposed deposition technique as a possible water based route for the preparation of flame retardant coatings based on nanoplates and bio-based components enabling environmental friendly processing.

### 2.3. Mechanical Properties Characterization

The mechanical properties of the uncoated and coated foams were assessed by compression test following the EN ISO 2439 standard procedure. Figure 7 reports the fourth compression cycle for PU, PU GO, and PU GO+DNA foams and a graphical representation of the compressive stress evaluated at 40% deformation. This latter parameter is normally referred as firmness and is correlated with the foam comfort.

The untreated open cell PU foam shows the typical three phases compressive/stress curve characterized by a linear elastic region (under 10% compression), a progressive buckling of the foam owing to cell collapsing and a final densification stage characterized by a steep increase of stress value after 50%

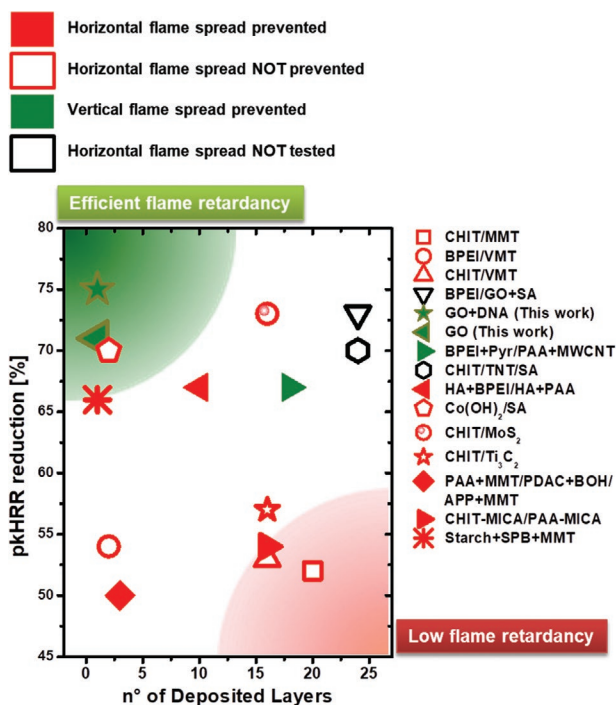


**Figure 6.** pkHRR reduction of GO and GO+DNA samples presented in this work and literature. Presented samples are referred to CHIT/MMT (chitosan/montmorillonite),<sup>[35]</sup> BPEI/VMT (branched polyethylenimine/vermiculite),<sup>[44]</sup> CHIT/VMT,<sup>[36]</sup> BPEI/GO+SA (SA is sodium alginate),<sup>[61]</sup> BPEI+Pyr/PAA+MWCNT (BPEI functionalized with pyrene/polyacrylic acid+ multiwalled carbon nanotubes),<sup>[54]</sup> CHIT/TNT/SA (TNT stay for titanate),<sup>[62]</sup> HA+BPEI/HA+PAA (HA stay halloysite),<sup>[63]</sup> Co(OH)<sub>2</sub>/SA,<sup>[64]</sup> CHIT/MoS<sub>2</sub>,<sup>[65]</sup> CHIT/Ti<sub>3</sub>C<sub>2</sub>,<sup>[66]</sup> PAA+MMT/PDAC+BOH/APP+MMT (PDAC and BOH stay for polydiallylammonium chloride and bohemite, respectively),<sup>[45]</sup> CHIT-MICA/PAA-MICA,<sup>[67]</sup> and Starch+SPB+MMT (SPB is sodium perborate).<sup>[68]</sup>

compression.<sup>[69]</sup> The treated foams show a similar behavior but the stress values are higher than what measured for the unmodified PU. The resulting curves still show the typical load/unload hysteresis curve of flexible PU thus suggesting

that the presence of the coating did not affect the ability of recovering the initial shape after being cyclically deformed. The observed behavior can be ascribed to both the rigid nature of a nanoplate containing coating and the strong electrostatic interactions occurring between the activation layer and the deposited GO.<sup>[40]</sup> The latter also confers a good structural stability to the coating upon multiple deformation cycles. The firmness of the GO and GO+DNA PU fall in the 4.5–5.5 kPa range (Figure 7b). Interestingly, the presence of DNA is responsible for a slight increase in this parameter thus further supporting the formation, upon deposition, of GO/DNA complexes characterized by ionic interactions. The calculated values indicate that the treated foams would behave similarly to high density (40–50 kg m<sup>-3</sup>) PU foams and might thus replace these latter in application fields such as transportation where flame retardant properties and weight reduction are mandatory.

### 3. Conclusion

In this paper, a single-step deposition approach based on graphene oxide and DNA has been developed to efficiently prepare PU foams characterized by high FR performances. This single-step deposition method was found capable of producing a homogeneous GO+DNA protective exoskeleton on the complex 3D structure of the foam. Interaction between GO and DNA may be ascribed to in situ formation of GO+DNA complexes upon drying of the coating, as denaturation of DNA may lead to uncompensated positive charges, observed to strongly bind to GO during a simple gelation experiment. The GO+DNA treated foams were capable of completely suppressing the melt dripping typical of PU foams and completely prevent flame spread during flammability tests in both horizontal and vertical configuration. Cone calorimetry tests further proved the ability of this GO+DNA coating to efficiently reduce combustion rates (–75% in pkHRR) while also releasing less smoke (–30% in TSR). Post combustion characterization pointed out the formation of expanded structures where GO platelets were likely expanded by the intrinsic intumescent behavior of DNA. This

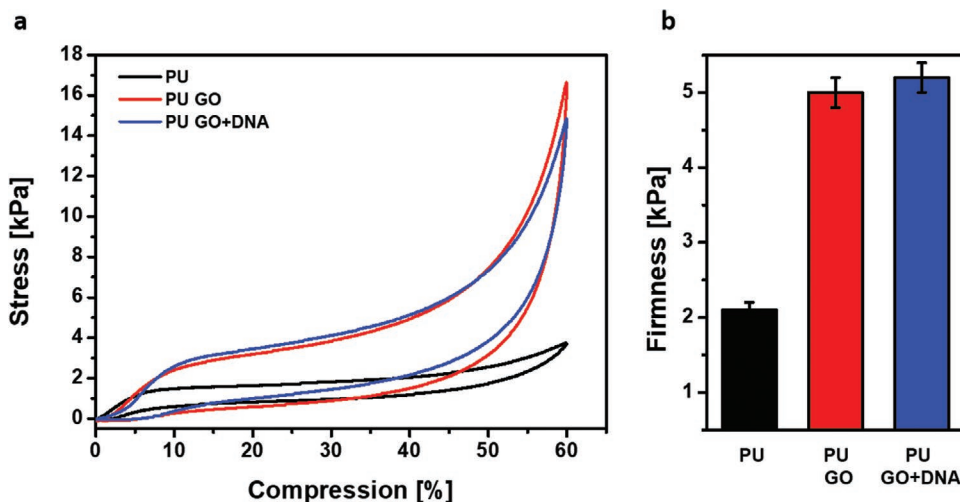


**Figure 7.** Mechanical characterization in compression mode of a) PU, PU GO, and PU GO+DNA samples and b) firmness calculation.



promoted the formation of a more efficient barrier toward heat and volatiles with respect to the coating only made of GO. A comparison with the literature background dealing with water-based FR coatings encompassing nanoparticles further highlighted the superior FR properties achieved by the developed GO+DNA coating.

In conclusion, the approach developed in this paper opens to the development of viable deposition routes encompassing graphene-related materials and bio-based flame retardants where processing efficiency and FR properties are optimized.

## 4. Experimental Section

**Materials:** Commercially available open cell polyurethane foams (density  $18 \text{ g dm}^{-3}$  and thickness 20 mm) were purchased by a local warehouse. PAA (average Mw 100 000, 35 wt%, in water), poly(diallyldimethylammonium chloride) sodium salt (PDAC, average Mw 400k–500k, 20 wt% in water), and deoxyribonucleic acid (DNA, powder, partially degraded) were purchased from Merck (Milan, Italy). PAA 1 wt% and PDAC 1 wt% solution were prepared with 18.2 M $\Omega$  ultrapure water supplied by a Q20 Millipore system (Milan, Italy). GO was purchased from AVANZARE Innovacion Tecnologica (Navarrete-La Rioja, Spain) as 1 wt% suspension in water. The description of GO synthesis was previously reported elsewhere.<sup>[42]</sup>

**Single-Step Deposition:** Prior deposition PU samples were cleaned by squeezing them several times in ultrapure water to remove processing residues and dust. Then, the PU samples were dried in oven at 80 °C, and the weight after water removal was considered as the starting one for the evaluation of the weight gain upon deposition. Specimens were activated by dipping in 1 wt% PAA solution followed by 1 wt% PDAC. The time was set to 10 min and after every dipping step, specimens were washed in ultrapure water by squeezing. The activation step is essential for the deposition of a homogeneous coating from nanoplates suspension. In fact, the first adsorption of PAA makes the PU surface negatively charged, favoring the deposition of the PDAC polycation molecules. PDAC acts as anchoring agent for GO and DNA which are negatively charged in water at room temperature conditions. Then, the activated foams were dried in oven at 80 °C for 2 h. The dried activated foams were placed in a handmade aluminum mold and the suspension of either 1 wt% GO or 1 wt% GO+0.1 wt% DNA or 0.1 wt% DNA was poured on the specimen filling its open porosity ( $2 \text{ mL cm}^{-2}$ ). Water was removed by drying the samples in oven at 80 °C overnight. The add-on % was calculated as the % of difference in weight after the treatment divided by the original dry weight of the foam and correspond to  $81 \pm 16\%$ ,  $87 \pm 4\%$ , and  $8 \pm 1\%$  for GO, GO+DNA, and DNA-treated foams, respectively. A schematic representation of the process is reported in Figure S1 (Supporting Information).

**Characterization:** The morphology of samples was investigated by FESEM (Zeiss Merlin 4248, Jena, Germany, beam voltage 5 kV). The samples were positioned on conductive tape and chromium sputtered prior to observation at beam voltage set to 5 kV.

Flammability test was performed on three samples for each coating formulation in both horizontal and vertical configuration by the application of a 20 mm blue methane flame for 3 s on the short size of the specimen ( $50 \times 150 \times 20 \text{ mm}^3$ ) positioned on a metallic grid (horizontal tests) or suspended with the aim of a clamp (vertical configuration). During combustion, the formation of molten incandescent polymer drops was evaluated by placing dry cotton underneath the samples. The final residues were evaluated by weighting the specimens before and after the test.

Forced combustion tests were performed on an oxygen consumption cone calorimeter (Fire Testing Technology, East Grinstead, UK) using  $50 \times 50 \times 20 \text{ mm}^3$  under  $35 \text{ kW m}^{-2}$  radiative flux. Measurements were performed three times for each formulation to obtain representative averages and experimental deviations. Raman spectra were performed

on an In Via Raman (Renishaw) equipped with a argon laser 514 nm/50 mW, 10 scans) coupled with a Leica DM 2500 optical microscope. D and G bands were fitted with Peak fit controller function from Origin 8.1 software applying Lorentzian functions. The cross section of the residues collected after cone calorimetry tests was investigated by SEM (Zeiss EVO 15, beam voltage 3 kV). The samples were cut in the center of the specimen and positioned on conductive tape and gold sputtered prior to observation.

Mechanical properties were evaluated on a dynamometer (Instron 5966, 2 kN cell, Canton, MA) by compressing two stacked samples of  $50 \times 50 \times 18 \text{ mm}^3$  between two horizontal plates and following the EN ISO 2439 standard (60% compression, deformation speed  $100 \text{ mm min}^{-1}$ ). The firmness was calculated as the stress at 40% deformation, according to ISO 3386 standard. Prior to the tests, samples were conditioned  $23.0 \pm 0.1 \text{ }^\circ\text{C}$  for 48 h at  $50.0\% \pm 0.1 \text{ RH}$  in a climatic chamber.

## Supporting Information

Supporting Information is available from the Wiley Online Library or from the author.

## Acknowledgements

The authors want to thank Mr. M. Raimondo, Mr. D. Pezzini, and Mr. F. Cuttica for FE-SEM and SEM imaging and cone calorimetry tests, respectively.

Open Access Funding provided by Politecnico di Torino within the CRUI-CARE Agreement.

## Conflict of Interest

The authors declare no conflict of interest.

## Author Contributions

F.C. and A.F. conceived the experiments, F.C. and A.F. coordinated the project, and F.C. and L.M. carried the deposition and the characterization. A.F., F.C., and L.M. contributed to the discussion and interpretation of the results. The manuscript was mainly written by L.M. and F.C.

## Data Availability Statement

Research data are not shared.

## Keywords

DNA, flame retardancy, graphene oxide, polyurethane foam, single-step deposition of flame retardant coating

Received: June 25, 2021

Revised: September 8, 2021

Published online: October 11, 2021

[1] M. Ahrens, *Home Fires That Began with Upholstered Furniture*, National Fire Protection Association, Quincy, MA **2008**.

[2] J. Lefebvre, B. Bastin, M. Le Bras, S. Duquesne, C. Ritter, R. Paleja, F. Poutch, *Polym. Test.* **2004**, *23*, 281.

- [3] E. D. Weil, S. V. Levchik, *J. Fire Sci.* **2004**, *22*, 183.
- [4] H. Singh, A. K. Jain, *J. Appl. Polym. Sci.* **2009**, *111*, 1115.
- [5] Y. Y. Chan, C. Ma, F. Zhou, Y. Hu, B. Schartel, *Polym. Degrad. Stab.* **2021**, 109656.
- [6] A. König, E. Kroke, *Fire Mater.* **2012**, *36*, 1.
- [7] F. Yang, G. L. Nelson, *Fire and Polymers VI: New Advances in Flame Retardant Chemistry and Science*, American Chemical Society, Washington, DC **2012**, pp. 139–149, Ch. 10.
- [8] G. Ming, S. Chen, Y. Sun, Y. Wang, *Combust. Sci. Technol.* **2017**, *189*, 793.
- [9] G. Malucelli, F. Carosio, J. Alongi, A. Fina, A. Frache, G. Camino, *Mater. Sci. Eng., R* **2014**, *84*, 1.
- [10] H. Sun, D. A. Schiraldi, D. Chen, D. Wang, M. Sánchez-Soto, *ACS Appl. Mater. Interfaces* **2016**, *8*, 13051.
- [11] O. Köklükaya, F. Carosio, L. Wågberg, *ACS Appl. Mater. Interfaces* **2017**, *9*, 29082.
- [12] Y.-T. Wang, H.-B. Zhao, K. Degracia, L.-X. Han, H. Sun, M. Sun, Y.-Z. Wang, D. A. Schiraldi, *ACS Appl. Mater. Interfaces* **2017**, *9*, 42258.
- [13] M. Ghanadpour, B. Wicklein, F. Carosio, L. Wågberg, *Nanoscale* **2018**, *10*, 4085.
- [14] O. Köklükaya, F. Carosio, V. L. Durán, L. Wågberg, *Carbohydr. Polym.* **2020**, *230*, 115616.
- [15] H.-B. Chen, D. A. Schiraldi, *Polym. Rev.* **2019**, *59*, 1.
- [16] N. Lavoine, L. Bergström, *J. Mater. Chem. A* **2017**, *5*, 16105.
- [17] G. Stieger, M. Scheringer, C. A. Ng, K. Hungerbühler, *Chemosphere* **2014**, *116*, 118.
- [18] Q. Wu, Q. Zhang, L. Zhao, S.-N. Li, L.-B. Wu, J.-X. Jiang, L.-C. Tang, *J. Hazard. Mater.* **2017**, *336*, 222.
- [19] Z.-R. Yu, M. Mao, S.-N. Li, Q.-Q. Xia, C.-F. Cao, L. Zhao, G.-D. Zhang, Z.-J. Zheng, J.-F. Gao, L.-C. Tang, *Chem. Eng. J.* **2021**, *405*, 126620.
- [20] H. Kim, D. W. Kim, V. Vasagar, H. Ha, S. Nazarenko, C. J. Ellison, *Adv. Funct. Mater.* **2018**, *28*, 1803172.
- [21] Q. Wu, L.-X. Gong, Y. Li, C.-F. Cao, L.-C. Tang, L. Wu, L. Zhao, G.-D. Zhang, S.-N. Li, J. Gao, Y. Li, Y.-W. Mai, *ACS Nano* **2018**, *12*, 416.
- [22] K.-Y. Guo, Q. Wu, M. Mao, H. Chen, G.-D. Zhang, L. Zhao, J.-F. Gao, P. Song, L.-C. Tang, *Composites, Part B* **2020**, *193*, 108017.
- [23] Q. Wu, J. Zhang, S. Wang, B. Chen, Y. Feng, Y. Pei, Y. Yan, L. Tang, H. Qiu, L. Wu, *Front. Chem. Sci. Eng.* **2021**, *15*, 969.
- [24] Q. Wu, C. Liu, L. Tang, Y. Yan, H. Qiu, Y. Pei, M. J. Sailor, L. Wu, *Soft Matter* **2021**, *17*, 68.
- [25] Z. Ma, X. Liu, X. Xu, L. Liu, B. Yu, C. Maluk, G. Huang, H. Wang, P. B. Song, *ACS Nano* **2021**, *15*, 11667.
- [26] D. Battagazzore, A. Frache, F. Carosio, *Composites, Part B* **2020**, *200*, 108310.
- [27] F. Carosio, M. Ghanadpour, J. Alongi, L. Wågberg, *Carbohydr. Polym.* **2018**, *202*, 479.
- [28] S. T. Lazar, T. J. Kolibaba, J. C. Grunlan, *Nat. Rev. Mater.* **2020**, *5*, 259.
- [29] P. Berndt, K. Kurihara, T. Kunitake, *Langmuir* **1992**, *8*, 2486.
- [30] H. L. Tan, M. J. McMurdo, G. Pan, P. G. Van Patten, *Langmuir* **2003**, *19*, 9311.
- [31] T. Soeno, K. Inokuchi, S. Shiratori, *Appl. Surf. Sci.* **2004**, *237*, 539.
- [32] S. Y. Park, M. F. Rubner, A. M. Mayes, *Langmuir* **2002**, *18*, 9600.
- [33] J. Choi, M. F. Rubner, *Macromolecules* **2005**, *38*, 116.
- [34] H. Yang, B. Yu, P. Song, C. Maluk, H. Wang, *Composites, Part B* **2019**, *176*, 107185.
- [35] G. Laufer, C. Kirkland, A. A. Cain, J. C. Grunlan, *ACS Appl. Mater. Interfaces* **2012**, *4*, 1643.
- [36] J. Lazar, F. Carosio, A.-L. Davesne, M. Jimenez, S. Bourbigot, J. Grunlan, *ACS Appl. Mater. Interfaces* **2018**, *10*, 31686.
- [37] S. Qin, M. G. Pour, S. Lazar, O. Köklükaya, J. Gerringer, Y. Song, L. Wågberg, J. C. Grunlan, *Adv. Mater. Interfaces* **2019**, *6*, 1801424.
- [38] L. Dong, J. Yang, M. Chhowalla, K. P. Loh, *Chem. Soc. Rev.* **2017**, *46*, 7306.
- [39] W. S. Hummers, R. E. Offeman, *J. Am. Chem. Soc.* **1958**, *80*, 1339.
- [40] L. Maddalena, J. Gomez, A. Fina, F. Carosio, *Nanomaterials* **2021**, *11*, 266.
- [41] L. Maddalena, F. Carosio, J. Gomez, G. Saracco, A. Fina, *Polym. Degrad. Stab.* **2018**, *152*, 1.
- [42] F. Carosio, L. Maddalena, J. Gomez, G. Saracco, A. Fina, *Adv. Mater. Interfaces* **2018**, *5*, 1801288.
- [43] B. Sang, Z.-W. Li, X.-H. Li, L.-G. Yu, Z.-J. Zhang, *J. Mater. Sci.* **2016**, *51*, 8271.
- [44] A. A. Cain, M. G. B. Plummer, S. E. Murray, L. Bolling, O. Regev, J. C. Grunlan, *J. Mater. Chem. A* **2014**, *2*, 17609.
- [45] F. Carosio, A. Fina, *Front. Mater.* **2019**, *6*, <https://doi.org/10.3389/fmats.2019.00020>.
- [46] J. D. Watson, F. H. C. Crick, *Nature* **1953**, *171*, 737.
- [47] Y. Xu, Q. Wu, Y. Sun, H. Bai, G. Shi, *ACS Nano* **2010**, *4*, 7358.
- [48] G. Malucelli, F. Bosco, J. Alongi, F. Carosio, A. Di Blasio, C. Mollea, F. Cuttica, A. Casale, *RSC Adv.* **2014**, *4*, 46024.
- [49] J. Alongi, F. Cuttica, A. D. Blasio, F. Carosio, G. Malucelli, *Thermochim. Acta* **2014**, *591*, 31.
- [50] J. Alongi, F. Cuttica, F. Carosio, *ACS Sustainable Chem. Eng.* **2016**, *4*, 3544.
- [51] J. Alongi, A. Di Blasio, J. Milnes, G. Malucelli, S. Bourbigot, B. Kandola, G. Camino, *Polym. Degrad. Stab.* **2015**, *113*, 110.
- [52] H. R. Horton, L. A. Moran, K. G. Scrimgeour, M. D. Perry, J. D. Rawn, *Principles of Biochemistry*, 4th ed., Pearson Education Inc, Prentice Hall, New Jersey, USA **2006**, pp. 852–852.
- [53] R. H. Krämer, M. Zammarano, G. T. Linteris, U. W. Gedde, J. W. Gilman, *Polym. Degrad. Stab.* **2010**, *95*, 1115.
- [54] K. M. Holder, A. A. Cain, M. G. Plummer, B. E. Stevens, P. K. Odenborg, A. B. Morgan, J. C. Grunlan, *Macromol. Mater. Eng.* **2016**, *301*, 665.
- [55] B. Schartel, T. R. Hull, *Fire Mater.* **2007**, *31*, 327.
- [56] A. C. Ferrari, D. M. Basko, *Nat. Nanotechnol.* **2013**, *8*, 235.
- [57] A. C. Ferrari, F. Bonaccorso, V. Fal'ko, K. S. Novoselov, S. Roche, P. Bøggild, S. Borini, F. H. L. Koppens, A. Palermo, N. Pugno, J. A. Garrido, R. Sordan, A. Bianco, L. Ballerini, M. Prato, E. Lidorikis, J. Kivioja, C. Marinelli, T. Ryhänen, A. Morpurgo, J. N. Coleman, V. Nicolosi, L. Colombo, A. Fert, M. Garcia-Hernandez, A. Bachtold, G. F. Schneider, F. Guinea, C. Dekker, M. Barbone, Z. Sun, C. Galiotis, A. N. Grigorenko, G. Konstantatos, A. Kis, M. Katsnelson, L. Vandersypen, A. Loiseau, V. Morandi, D. Neumaier, E. Treossi, V. Pellegrini, M. Polini, A. Tredicucci, G. M. Williams, B. Hee Hong, J.-H. M. Ahn, J. Kim, H. Zirath, B. J. van Wees, H. van der Zant, L. Occhipinti, A. Di Matteo, I. A. Kinloch, T. Seyller, E. Quesnel, X. Feng, K. Teo, N. Rupesinghe, P. Hakonen, S. R. T. Neil, Q. Tannock, T. Löfwander, J. Kinaret, *Nanoscale* **2015**, *7*, 4598.
- [58] C. Backes, A. M. Abdelkader, C. Alonso, A. Andrieux-Ledier, R. Arenal, J. Azpeitia, N. Balakrishnan, L. Banszerus, J. Barjon, R. Bartali, S. Bellani, C. Berger, R. Berger, M. M. B. Ortega, C. Bernard, P. H. Beton, A. Beyer, A. Bianco, P. Bøggild, F. Bonaccorso, G. B. Barin, C. Botas, R. A. Bueno, D. Carriazo, A. Castellanos-Gomez, M. Christian, A. Ciesielski, T. Ciuk, M. T. Cole, J. Coleman, C. Coletti, L. Crema, H. Cun, D. Dasler, D. De Fazio, N. Díez, S. Drieschner, G. S. Duesberg, R. Fasel, X. Feng, A. Fina, S. Forti, C. Galiotis, G. Garberoglio, J. M. García, J. A. Garrido, M. Gibertini, A. Götzhäuser, J. Gómez, T. Greber, F. Hauke, A. Hemmi, I. Hernandez-Rodriguez, A. Hirsch, S. A. Hodge, Y. Huttel, P. U. Jepsen, I. Jimenez, U. Kaiser, T. Kaplas, H. Kim, A. Kis, K. Papagelis, K. Kostarelos, A. Krajewska, K. Lee, C. Li, H. Lipsanen, A. Liscio, M. R. Lohe, A. Loiseau, L. Lombardi, M. F. López, O. Martín, C. Martín, L. Martínez, J. A. Martín-Gago, J. I. Martínez, N. Marzari, Á. Mayoral, J. McManus, M. Melucci, J. Méndez, C. Merino, P. Merino, A. P. Meyer,

- E. Miniussi, V. Miseikis, N. Mishra, V. Morandi, C. Munuera, R. Muñoz, H. Nolan, L. Ortolani, A. K. Ott, I. Palacio, V. Palermo, J. Parthenios, I. Pasternak, A. Patane, M. Prato, H. Prevost, V. Prudkovskiy, N. Pugno, T. Rojo, A. Rossi, P. Ruffieux, P. Samori, L. Schué, E. Setijadi, T. Seyller, G. Speranza, C. Stampfer, I. Stenger, W. Strupinski, Y. Svirko, S. Taioli, K. B. K. Teo, M. Testi, F. Tomarchio, M. Tortello, E. Treossi, A. Turchanin, E. Vazquez, E. Villaro, P. R. Whelan, Z. Xia, R. Yakimova, S. Yang, G. R. Yazdi, C. Yim, D. Yoon, X. Zhang, X. Zhuang, L. Colombo, A. C. Ferrari, M. Garcia-Hernandez, *2D Mater.* **2020**, *7*, 022001.
- [59] C. Sheng, *Fuel* **2007**, *86*, 2316.
- [60] A. Yoshida, Y. Kaburagi, Y. Hishiyama, *Carbon* **2006**, *44*, 2333.
- [61] H. Pan, B. Yu, W. Wang, Y. Pan, L. Song, Y. Hu, *RSC Adv.* **2016**, *6*, 114304.
- [62] H. Pan, W. Wang, Y. Pan, L. Song, Y. Hu, K. M. Liew, *ACS Appl. Mater. Interfaces* **2015**, *7*, 101.
- [63] R. J. Smith, K. M. Holder, S. Ruiz, W. Hahn, Y. Song, Y. M. Lvov, J. C. Grunlan, *Adv. Funct. Mater.* **2018**, *28*, 1703289.
- [64] X. Mu, B. Yuan, Y. Pan, X. Feng, L. Duan, R. Zong, Y. Hu, *Mater. Chem. Phys.* **2017**, *191*, 52.
- [65] H. Pan, Q. Shen, Z. Zhang, B. Yu, Y. Lu, *J. Mater. Sci.* **2018**, *53*, 9340.
- [66] B. Lin, A. C. Y. Yuen, A. Li, Y. Zhang, T. B. Y. Chen, B. Yu, E. W. M. Lee, S. Peng, W. Yang, H.-D. Lu, Q. N. Chan, G. H. Yeoh, C. H. Wang, *J. Hazard. Mater.* **2020**, *381*, 120952.
- [67] A. Fahami, J. Lee, S. Lazar, J. C. Grunlan, *ACS Appl. Mater. Interfaces* **2020**, *12*, 19938.
- [68] R. Davis, Y.-C. Li, M. Gervasio, J. Luu, Y. S. Kim, *ACS Appl. Mater. Interfaces* **2015**, *7*, 6082.
- [69] W. N. Patten, S. Sha, C. A. Mo, *J. Sound Vib.* **1998**, *217*, 145.